

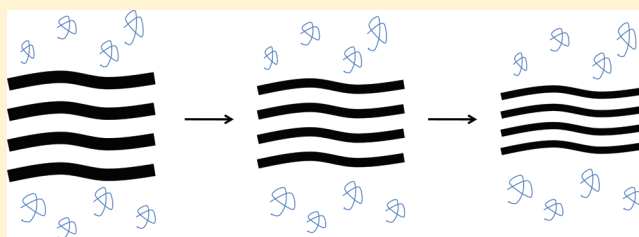
# Effect of Temperature on the Interactions between Dipolar Membranes

Pablo Szekely,<sup>†,‡</sup> Roi Asor,<sup>†</sup> Tom Dvir,<sup>†,‡</sup> Or Szekely,<sup>†</sup> and Uri Raviv<sup>\*,†</sup>

<sup>†</sup>The Institute of Chemistry and <sup>‡</sup>The Racah Institute of Physics, The Hebrew University of Jerusalem, Edmond J. Safra Campus, Givat Ram, 91904 Jerusalem, Israel

## Supporting Information

**ABSTRACT:** It is well-known that phospholipids in aqueous environment self-assemble into lamellar structures with a repeat distance governed by the interactions between them. Yet, the understanding of these interactions is incomplete. In this paper, we study the effect of temperature on the interlamellar interactions between dipolar membranes. Using solution small-angle X-ray scattering (SAXS), we measured the repeat distance between 1,2-dilauroyl-*sn*-glycero-3-phosphocholine (DLPC) bilayers at different temperatures and osmotic stresses. We found that when no pressure is applied the lamellar repeat distance,  $D$ , decreases and then increases with increasing temperature. As the osmotic stress increases,  $D$  decreases with temperature and then increases to a limited extent, until at sufficiently high pressure  $D$  decreases with temperature in all the examined range. We then reconstructed experimentally the equation of state and fit it with a modified interaction model that takes into account the temperature dependence of the fluctuation term. Finally, we showed how the thickness of DLPC membranes decreases with temperature.



## INTRODUCTION

The interactions between phospholipid membranes are crucial for understanding their self-assembly processes when added to water.<sup>1</sup> In excess of water, phospholipids usually self-assemble into bilayers that form vesicles, which resemble biological membranes. Such membranes often form a collection of multilamellar vesicles (MLVs). At low water concentration, lipids may assume different structures and phases such as cylindrical rodlike phases, bicontinuous phases, or micelles.<sup>1</sup> The interactions between the membranes define their equilibrium repeat distance,  $D$ , within the MLV structure. Several forces contribute to the total interaction between membranes: the attractive van der Waals forces,<sup>1</sup> which result from dispersion interaction between any two objects; the repulsive hydration forces<sup>2,3</sup> that emerge from the energetic cost of displacing the last few aqueous layers between interacting molecules; the entropic repulsive undulation forces,<sup>3</sup> associated with thermal fluctuations; and the electrostatic forces.<sup>4</sup> The electrostatic interaction is relevant when the membranes are charged; a property that depends on the structure and charge of the lipid headgroup.

Even between neutral membranes, the complexity of the interactions leads to nontrivial thermodynamic phenomena. The equations of state of several dipolar (net neutral) membranes, composed of lipids with zwitterionic headgroups, were measured.<sup>3,5</sup> The data were analyzed and concurred with the theoretical predictions, described in the following section. To better understand the thermodynamics of dipolar membranes, it is essential to study the effect of temperature on those interactions. The temperature can influence the

magnitude and character of each one of the contributing forces to the total interaction and the balance between them.

It is well-known that lipid membranes have a temperature-dependent phase transition;<sup>6–8</sup> below the melting temperature ( $T_m$ ) the lipids are better organized in an all-trans configuration within the bilayer. This organization limits the lateral thermal motion of the lipids and stiffens the membranes. Below  $T_m$  the membrane is in a lamellar liquid crystalline gel phase (called  $L_\beta$  phase). Above  $T_m$  the membranes are in the liquid phase (called  $L_\alpha$  phase), which is much softer because the lipid tails achieve a cis–trans configuration, the area per headgroup increases, and the lipid molecules are free to flow within the membrane almost like a two-dimensional fluid.<sup>1</sup> This feature has a crucial biological importance where, for example, raft domains of a gel-phased lipid “float” in a “sea” of lipids in the liquid phase whereas cholesterol is often used to stiffen the membranes when needed.<sup>9</sup>

In this paper, we present the experimental isotherms of dipolar membranes at their liquid phase and suggest empirical adjustments to earlier theoretical expressions to account for our observations. We then present an experimental method, based on solution X-rays scattering, for estimating the thickness of tightly packed membranes (as opposed to weakly coupled bilayers<sup>10</sup>).

**Received:** September 22, 2011

**Revised:** February 18, 2012

**Published:** February 21, 2012

## ■ EXPERIMENTAL METHODS

Lyophilized 1,2-dilauroyl( $C_{12:0}$ )-*sn*-glycero-3-phosphocholine (DLPC) and 1,2-dioleoyl-*sn*-glycero-3-phosphocholine (DOPC) were purchased from Avanti Polar Lipids, Inc., AL. We chose to work with DLPC as it forms bilayers that are softer than most other lipids.<sup>11</sup> In other words, the bending rigidity of DLPC is low compared with other bilayers made of other lipids found in cells.<sup>12,13</sup> Hence the contribution of the undulation interaction, between DLPC bilayers, to the total interaction is significant.

We added highly purified water (Barnstead Nanopure Diamond)<sup>14,15</sup> to lyophilized DLPC to obtain lipid solutions at the required final weight concentration of 30 mg/(mL of water). Each lipid solution was vortex mixed for an hour in an eppendorf tube. All the preparation and measurements of the lipids were done above the melting temperature of the membranes.<sup>16</sup>

Solutions of poly(ethylene glycol) (PEG), molecular weight 20 000 g/mol (purchased from Sigma), were prepared at various weight percents (0%, 0.2%, 1%, 1.5%, 2%, 4%, 6%, 14%, 20%, and 30%) by adding highly purified water (Barnstead Nanopure Diamond) to the PEG powder. We used PEG as it is a highly water-soluble uncharged polymer in all the used temperature range (as shown by osmotic stress measurements<sup>17</sup>) and does not interact with the lipid bilayers. The energy cost for this PEG chain to penetrate into the multilamellar vesicle is approximately  $8\text{--}14 k_B T$ , for a typical water gap of 2–3 nm between bilayers (see Supporting Information). Most of the chains should therefore remain outside the lamellar phase.

Equal volumes from the lipid and PEG solutions were vortex mixed and transferred into a quartz capillary. The mixture was centrifuged at a relative centrifugal force (RCF) of 1780g for 3 min at ambient room temperature, using a Thermo IEC Centra CL2 centrifuge equipped with a 15 mL tube rotor, and flamed sealed. The sealed samples were then centrifuged at RCF of 6000g, using a Sigma 1-15PK centrifuge equipped with rotor No. 11024, suitable for capillaries.

Using high-resolution solution small-angle X-ray scattering (SAXS), described earlier,<sup>18–20</sup> we determined the repeat distance,  $D$ , of the lamellar phases. The measurements were performed in a temperature-controlled sample chamber (Xryovn, Forvis Technologies Inc., Santa Barbara, CA) with 0.01 °C accuracy. After each temperature change, we waited for ca. 90 min to let the solution equilibrate at the new temperature. We ensured that this period is sufficient for the solutions to reach equilibrium by measuring some of the samples repeatedly during the first 300 min after a temperature change of a few degrees. Fifteen minutes following the temperature change, the repeat distance stabilized. Using the analysis software, X+, developed in our laboratory,<sup>19</sup> we analyzed the structure factors of the radially integrated scattering curves (Figures S1 and S2 in the Supporting Information).

An osmotic pressure was matched for each PEG concentration and temperature.<sup>17</sup> That pressure agreed well with our own osmotic stress measurements, using a vapor pressure osmometer (Vapro 5520 Wescor, Inc.) as described.<sup>10,21</sup> The data were fit to the expected interactions while the temperature at which each datum was measured was fixed and the membrane thickness,  $\delta$ , was the only free parameter in the interaction model.

## ■ MODELING THE INTERACTION BETWEEN NEUTRAL MEMBRANES

The van der Waals (vdW) free energy per unit area,  $f_{\text{vdW}}$ , results from the interactions between induced and permanent dipoles within and across bilayers.  $f_{\text{vdW}}$  is the only attractive interaction and is described by

$$f_{\text{vdW}}(d_W, T) = -\frac{H(T)}{12\pi} \left( \frac{1}{d_W^2} - \frac{2}{(d_W + \delta)^2} + \frac{1}{(d_W + 2\delta)^2} \right) \quad (1)$$

$H$  is the Hamaker coefficient,  $d_w$  is the water spacing between the membranes,<sup>22</sup> and  $\delta$  is the membrane thickness.<sup>23</sup>  $H$  has an explicit expression<sup>1,24</sup>

$$H(T) \cong \frac{3k_B T}{2} \sum_0^\infty \left( \frac{\epsilon_w - \epsilon_m}{\epsilon_w + \epsilon_m} \right)^2 R_n(\delta, d_w) \quad (2)$$

where  $R_n$  are the retardation terms.  $\epsilon_w$  and  $\epsilon_m$  are the dielectric constants of water and the membranes, respectively. The temperature dependence of the water dielectric constant was also taken into account using the relation<sup>1</sup>  $\epsilon_w(T_2) = [\epsilon_w(T_1)](T_2/T_1)^{-1.36}$ , where  $\epsilon_w(298 \text{ K}) = 78$ , and was found to have an indistinguishable effect on the total interaction. The summation was empirically found to be of order unity.

The hydration interaction is short-range and describes the energy needed for displacing the last few water molecules between the membranes. The dielectric constant between the membranes should drop from about 78 in water to about 5 upon removing the last hydration shell. At low dielectric constant, the Born self-energy of the ions composing the zwitterionic DLPC headgroups rises and considerably destabilizes the bilayers.<sup>1</sup> The hydration interaction term is basically a steric or geometric limitation of the system. Experimentally, the free energy per unit area was found<sup>25</sup> to be

$$f_{\text{hyd}}(d_W) = H_0 e^{-d_w/\lambda_h} \quad (3)$$

where  $H_0 \approx 4k_B T/\text{\AA}^2$  and  $\lambda_h$  is a typical microscopic hydration range of order  $\sim 2 \text{ \AA}$ .

The undulation interaction (also called the Helfrich interaction) is a repulsive interaction associated with the membrane entropic thermal fluctuations. As bilayers in the lamellar phase get closer, their thermal fluctuations are restricted (by the surrounding bilayers) and their entropy decreases. Recent correction in this term led to the following empirical expression<sup>3</sup>

$$f_{\text{und}}(d_W, T) = \frac{(kT)^2 A_{\text{fl}}}{4\pi^2 K_c} \exp(-d_w/\lambda_{\text{fl}}) \quad (4)$$

For DLPC at room temperature,  $\lambda_{\text{fl}}$  is 6 Å and  $A_{\text{fl}}$  is 1.06 Å<sup>-2</sup>. Many empirical values were reported<sup>23</sup> for  $A_{\text{fl}}$  and they are all within an error of  $\pm 20\%$ . The effect of temperature on those parameters, however, was not studied.  $K_c$  is the membrane bending rigidity and strongly depends on the membrane thickness,  $\delta$ , and the area per headgroup,  $a$ , and follows the relation:  $K_c \propto \delta^\beta a^{-\alpha}$  where  $\alpha = 8$  and  $\beta = 3.2$ .<sup>26</sup> We tried several values for  $\alpha$  and  $\beta$ , and discovered that the dependence of the estimated  $\delta$  on the values of  $\alpha$  and  $\beta$  is weak (Figure S3 in the

Supporting Information) and the values are in agreement with earlier studies on similar membranes.<sup>10,27</sup>

We neglected the electrostatic interaction between the neutral DLPC bilayers, as varying the concentration of added NaCl had a negligible effect on the spacing between DLPC and other bilayers consisting of lipids with PC headgroups.<sup>3,12</sup>

In order to obtain the pressure,  $P(d_w, T)$ , we derived the total interaction per unit area

$$f = f_{\text{vdW}} + f_{\text{hyd}} + f_{\text{und}} \quad (5)$$

with respect to  $d_w$

$$P(d_w, T) = - \frac{\partial f(d_w, T)}{\partial d_w} \quad (6)$$

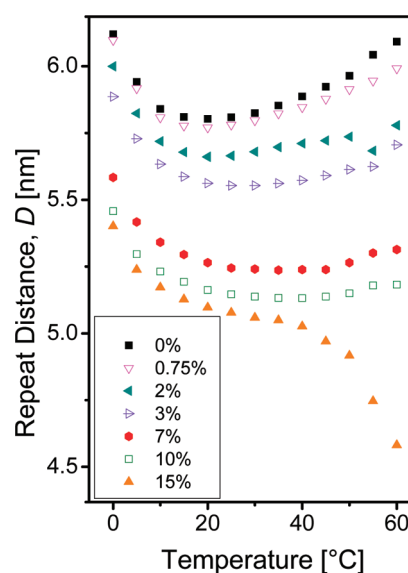
This summation of the main attractive and repulsive interactions (eq 5) leads to an equilibrium repeat distance where the neutral membranes achieve a minimal energy value. If the membranes get farther apart, they feel vdW attraction, and they are repelled by the hydration and undulation interactions if they get closer. At the very last few water layers the hydration interaction dominates.

## RESULTS

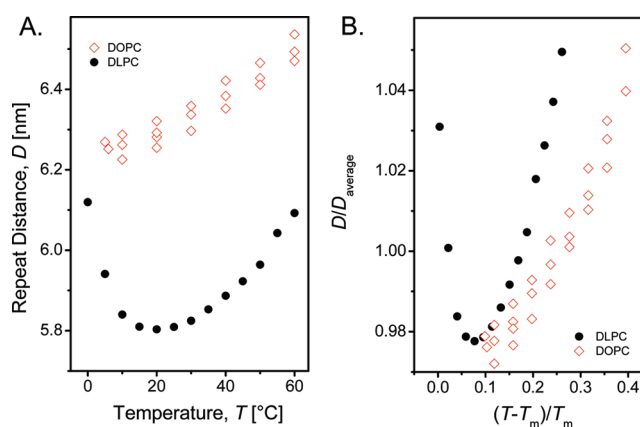
Using small-angle X-ray scattering (SAXS) setup, we measured the scattering of 15 mg/mL DLPC solutions at different PEG concentrations (Figure S1 in the Supporting Information). We then radially integrated the scattering intensity,  $I$ , as a function of the magnitude of the momentum transfer vector,  $q$ , and obtained the scattering profiles (Figure S2 in the Supporting Information). From the center of the scattering correlation peaks, we found the repeat distance of the lamellar phase, under different osmotic pressures. We repeated the measurements several times at different temperatures,  $T$ , and obtained pressure–distance isotherms. Each isotherm was fit to an interaction curve using the model presented above (eq 6). Repeated heating and cooling cycles verified the reversibility of the results up to 60 °C.

Figure 1 shows the DLPC lamellar repeat distance,  $D$ , as function of  $T$  at each PEG concentration. The results indicate that when no osmotic pressure is applied to DLPC membranes (i.e., when no PEG is added),  $D$  decreases with the temperature until it reaches a minimum somewhere between 20 and 30 °C. At higher temperatures, the lamellar phase swells with increasing temperature due to stronger thermal fluctuations. The added PEG solutions apply pressure to the DLPC membranes, suck the water between them, and the  $D(T)$  curves assume lower values (as expected). At high pressures, the swelling part of the  $D(T)$  curve is much smaller and at the highest pressure  $D$  only decreases with temperature. We qualitatively explain this behavior by the decrease in thermal fluctuations as the osmotic stress increases.

Figure 2A compares the repeat distances,  $D$ , of DLPC membranes with those of DOPC membranes. At the relevant temperature range,  $D$  of DOPC monotonically increases but at a lower rate than  $D$  of DLPC. Normalizing the repeat distance by the average repeat distance,  $D_{\text{av}}$ , and the temperature by the melting temperature of the gel phase,  $T_m$ , clarifies the effect (Figure 2B). DOPC is thicker and its bending rigidity is higher than that of DLPC.<sup>12</sup> The DOPC undulation interaction term has therefore a smaller contribution to the total interaction between DOPC bilayers. This result strengthens our assumption that the increase of the repeat distance at higher



**Figure 1.** Repeat distance,  $D$ , of DLPC as a function of temperature,  $T$ . Different symbols represent different poly(ethylene glycol) (PEG) weight percents, as indicated in the figure.



**Figure 2.** (A) Repeat distance,  $D$ , of DLPC (black solid circles) and DOPC (red open diamonds) as a function of temperature,  $T$ , when no PEG is added. (B) The same data are plotted using dimensionless variables.  $D_{\text{av}}$  is the mean value of  $D$  for each lipid, averaged over all temperatures.  $T_m$  is the melting temperature of each lipid.

temperatures originates from the undulation interaction. An earlier study with DOPC reported the bending rigidity, the total interaction, and the bilayer structure at different temperatures and is in line with our results.<sup>28</sup>

By presenting the osmotic pressure, applied to the DLPC bilayers, as a function of  $D$ , we obtained the thermodynamic classical isotherms of DLPC membranes (Figure 3). The model described above could not fit any of the isotherms. In order to fit the isotherms, we had to slightly modify the model. The data suggest that the entropic thermal fluctuations should significantly increase with  $T$ ; hence the interaction range of  $f_{\text{und}}$ , determined by  $\lambda_{\text{fl}}$ , should accordingly increase. We imposed an empirical linear ( $a_{\text{fl}}T + b_{\text{fl}}$ ) dependence of  $\lambda_{\text{fl}}$  on the thermal energy,  $k_B T$ . At  $T = 0$  there are no thermal fluctuations, and hence  $b_{\text{fl}}$  should be close to zero. The slope,  $a_{\text{fl}}$ , was calibrated by using the known value of  $\lambda_{\text{fl}}$  at room

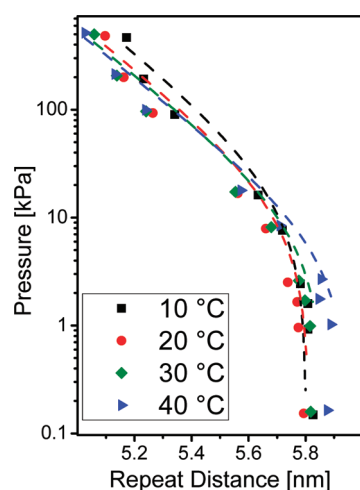


**Figure 3.** Pressure–repeat distance curves of DLPC in water, at different temperatures, as indicated in the figure. The data (symbols) are taken from Figure 1. The corresponding broken curves (in similar colors) are the calculated pressures, using our modified model (see text).

temperature.<sup>3</sup> These considerations lead to the following simple expression

$$\lambda_{\text{fl}}(T) = \frac{\lambda_{\text{fl}}(T_{\text{room}})T}{T_{\text{room}}} \quad (7)$$

This empirical relation reproduces the data and most importantly the crossing of the isotherms, which means that unless another variable exists the equation of state is surjective (i.e., not a one-to-one relation) (Figure 3). Repeating the fitting process with different  $\alpha$  and  $\beta$  parameters for the bending rigidity ( $K_c \propto \delta^{\beta} a^{-\alpha}$ ) gave similar values of  $\delta$  (Figure S3 in the Supporting Information), suggesting that the major contribution to the undulation forces originates in the exponent term of eq 4. The pressure–distance isotherm curves, however, were more sensitive to the values of  $\alpha$  and  $\beta$ . Unlike the theoretically predicted<sup>26</sup> values of  $\alpha = 7-8$  and  $\beta = 3.2$ , we found that  $\alpha = 0$  and  $\beta = 3.2$  best fit the data (Figure 3).

In the interaction model, the only free parameter is the effective interaction membrane thickness,  $\delta$ , of the DLPC membranes. From each curve, we extracted the best-fitting effective interaction membrane thickness. The theoretical curves stopped fitting the experimental data from 50 °C, where a sudden drop in the repeat distance appears (Figure 1). We find that  $\delta$  decreases with increasing temperature (Figure 4).

Another method to measure the membrane thickness is Luzzati's gravimetric or volumetric method.<sup>29</sup> This method requires very high lipid volume fractions,  $\phi$ , at which the membranes repel one another and fill out the entire available space. The repeat distance,  $D$ , between them is then given by  $D = \delta/\phi$ . The assumption here is that all the water resides between bilayers. It is known, however, that the lipids form multilamellar vesicles.<sup>30</sup> Yet, a qualitatively similar result was obtained when the X-ray scattering form factors of DLPC in solution of 10 mM  $\text{CaCl}_2$  were analyzed and the head-to-head<sup>31</sup> membrane thickness as well as the corresponding Luzzati thickness were obtained (Figure 4). Those experiments were described and discussed elsewhere.<sup>10</sup> The lower values of the two other methods (Figure 4) result from the fact that both give lower bounds to the actual membrane thickness<sup>10</sup> whereas

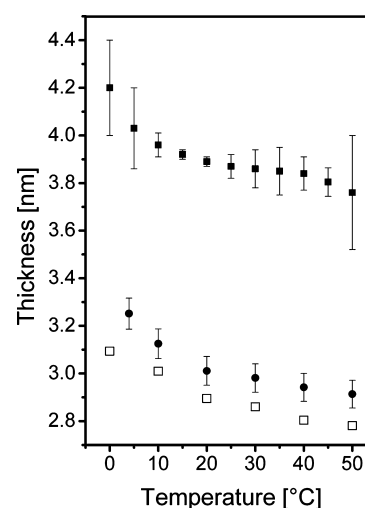


**Figure 4.** Effective membrane interaction thicknesses,  $\delta$ , as a function of temperature (solid square symbols), extracted from the fit of the pressure–distance isotherms (Figure 3). For comparison, we show the membrane thickness obtained by volumetric method (open square symbols) and by X-ray scattering form-factor analysis, which gave the head-to-head bilayer thickness (solid circles).<sup>10</sup> These measurements agree with earlier studies.<sup>27,30</sup>

the effective interaction membrane thickness provides an upper bound for the membrane thickness. In whatever way we measured the thickness, it always decreased with increasing temperature, in agreement with earlier reports.<sup>30</sup>

## DISCUSSION

To fit the data in Figure 3 we modified the undulation interaction term of our model by assuming that the typical range of the undulation interaction,  $\lambda_{\text{fl}}$ , linearly grows with the temperature. The unmodified model was confirmed for DLPC at ambient room temperature.<sup>3</sup> In the earlier study,<sup>3</sup> the classical Helfrich power law undulation interaction term was replaced by an exponential dependence and the value for  $\lambda_{\text{fl}}$  was experimentally found at ambient room temperature.

We also used the earlier<sup>3,25</sup> values for the hydration interaction term and found<sup>10</sup> that the thickness of charged membranes decreases with increasing temperature. NMR<sup>32,33</sup> studies addressed this issue as well and found similar thickness temperature dependence with dipolar (zwitterionic) membranes. At higher temperatures there is a higher lipid-tail entropy that increases the area per headgroup,<sup>10</sup> and leads to conformational changes of the tails that thin the membrane, with increasing temperature, in order to avoid contact with the aqueous solution.

The data in Figure 1 already suggest the relative contribution of each term, in eq 5, to the total interaction between the membranes at each temperature. A decrease of the lamellar repeat distance,  $D$ , is expected as the vdW interaction linearly strengthens with the temperature. Close to the melting temperature of DLPC (−1 °C), an anomalous pretransition may take place and account for some of the increase of the membrane thickness when lowering the temperature.<sup>34</sup> A qualitative analysis shows that the degree of divergence of the membrane thickness is much less than the divergence of  $D$  or of the water gap between bilayers. Even at high osmotic pressures, the anomalous divergence in  $D$ , close to the lipid melting point is primarily due to the anomalous divergence of the water layer thickness.<sup>30</sup> The data at zero or low osmotic stress suggest that



the undulation term increases with temperature more than the linearly increasing vdW term does, as at some point the repulsion overcomes the attractive vdW interaction and  $D$  increases. The undulation term emerges from the entropic fluctuations between the membranes. Therefore, the osmotic pressure applied by the PEG molecules should mainly affect the undulation term. The fact that addition of PEG suppresses the increase of  $D$ , observed at low pressures, suggests that the undulations are strongly suppressed. At sufficiently high osmotic stress the vdW attraction dominates and  $D$  decreases in all the measured temperature range (Figure 5).

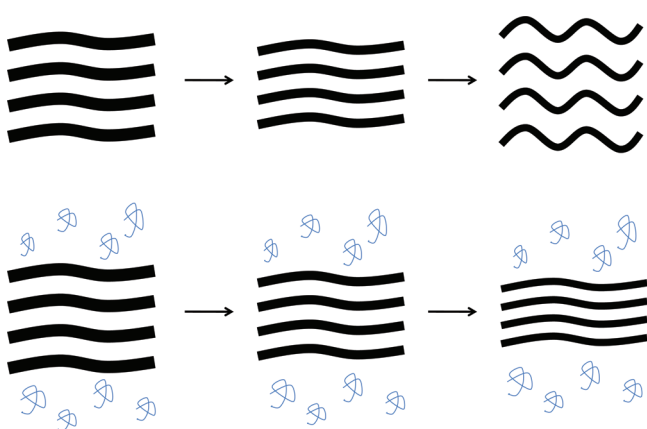


**Figure 5.** An illustration of a possible qualitative explanation of the observed behavior (Figure 1): without PEG the membranes initially get closer but then, as the temperature increases, thermal fluctuations dominant and the membranes separate (top). The addition of PEG polymer molecules (shown in blue) suppresses the fluctuations and the lamellar repeat distances decreases with temperature due to bilayer thinning and stronger vdW attraction (bottom). The arrows represent a temperature rise.

Another possible explanation for the sharp decrease in the repeat distance,  $D$ , at low temperatures (<ca. 4 °C) could be linked to the critical stretching of the bilayer around the liquid–gel phase transition, which for DLPC occurs at −1 °C.<sup>6</sup> Usually the typical temperature range, in which the bilayers stretch, is quite narrow and the vast majority of the anomalous bilayer thickness divergence effect is confined to within 4 °C around the phase transition temperature.<sup>34,35</sup> It is possible that the data points measured at 0 °C are still affected by anomalous divergence of bilayer thickness. For the other data points ( $T \geq 5$  °C) the effect of anomalous divergence of bilayer thickness is expected to be irrelevant.<sup>30</sup> Note that the increase in the bilayer thickness at these low temperatures (Figure 4) does not account for all the measured variation in the repeat distance,  $D$ , which we attribute to the water layer (Figure 1).<sup>30</sup> The decrease of  $D$  with  $T$  near  $T_m$  could be explained by the decrease of the bending rigidity close to the transition temperature.<sup>36</sup>

When trying to fit the data with the equations described above, without any membrane thickness adjustments, the fits were poor and did not predict the behavior of the DLPC membranes. We then found that the membrane thickness is a very sensitive fitting parameter. From 50 °C, the curves could not fit the data well, suggesting that under those conditions, other interaction parameters, reported at room temperature,<sup>3</sup> may vary at those high temperatures.

The thickness extracted from the fit is a property of the DLPC membrane but differs from the volumetric or head-to-

head thicknesses<sup>31</sup> (Figure 4). The thickness we found is the effective interaction membrane thickness or steric interaction thickness. Luzzati's volumetric thickness and the head-to-head thicknesses behave in a similar manner as the steric thickness; both decrease at a similar rate with temperature,<sup>10</sup> yet Luzzati's volumetric and the head-to-head thicknesses are ca. 0.8–1 nm thinner than the steric thickness. The steric thickness corresponds to the plan from which the interactions are measured, and probably includes some part of the hydration layers around the opposing lipid headgroups, whereas the Luzzati thickness corresponds to the dry bilayer thickness, assuming that all the water added to the system contributes to the interlamellar spacing, and is an approximation that is a lower bound for any membrane thickness.

The undulations in real biological membranes are probably suppressed by the presence of cholesterol and membrane proteins that stiffen the membranes. Our study was done on softer membranes and highlights the effect of thermal fluctuations on the structure of membranes. This might be the case locally in some membranous domains. Biological bilayers are likely to adopt structures and interactions that correspond to the osmotic stress in their environment, as this study suggests.

## CONCLUSIONS

In this paper, we characterized the interactions between dipolar DLPC membranes, and suggested new insights based on the behavior of the membranes at different temperatures. We discovered an unusual crossing of isotherms. By assuming that the fluctuation parameter,  $\lambda_H$ , is increasing linearly with temperature, we can fit the data well and reproduce the isotherm crossing and obtain the effective interaction membrane thickness. We found that osmotic stress can strongly suppress the thermal fluctuations between the membranes and that at high osmotic pressure the vdW interaction dominates. From 50 °C and at high PEG concentrations the suggested model breaks, suggesting that other interaction parameters vary with pressure and temperature.

## ASSOCIATED CONTENT

### Supporting Information

Examples of raw X-ray data, integrated scattering curves, and data analysis, as well as estimation for the energy cost for the PEG chain to penetrate into the multilamellar vesicles, and the temperature dependence of the interaction thickness on the assumed power laws  $K_c \propto \delta^\beta a^{-\alpha}$ . This material is available free of charge via the Internet at <http://pubs.acs.org>.

## AUTHOR INFORMATION

### Corresponding Author

\*E-mail: [raviv@chem.huji.ac.il](mailto:raviv@chem.huji.ac.il). Tel: +972-2-6586030. Fax: +972-2-5618033.

### Notes

The authors declare no competing financial interest.

## ACKNOWLEDGMENTS

We thank D. Harries for helpful discussions. This project was supported by the Israel Science Foundation and the James Frank program. P.S. and O.S. acknowledge support from the Samuel and Lottie Rudin Foundation fellowships. T.D. acknowledges support from a short-term fellowship of The

Institute of Chemistry and the Faculty of Mathematics and Sciences at The Hebrew University. R.A. and T.D. thank the nanocenter of the Hebrew University for fellowship support. We thank the Safra, Wolfson, and Rudin Foundations for supporting our laboratory.

## ■ REFERENCES

- (1) Israelachvili, J. N. *Intermolecular and Surface Forces*, 2nd ed.; Academic Press: New York, 1992.
- (2) Rand, R. P.; Parsegian, V. A. *Biochim. Biophys. Acta* **1989**, *988*, 351.
- (3) Petrache, H. I.; Tristram-Nagle, S.; Harries, D.; Kucerka, N.; Nagle, J. F.; Parsegian, V. A. *J. Lipid Res.* **2006**, *47*, 302.
- (4) Andelman, D. Electrostatic Properties of Membranes: The Poisson–Boltzmann Theory. In *Handbook of Biological Physics*; Elsevier Science B.V.: Amsterdam, 1995; pp 603.
- (5) Leontidis, E.; Aroti, A.; Belloni, L.; Dubois, M.; Zemb, T. *Biophys. J.* **2007**, *93*, 1591.
- (6) Mabrey, S.; Sturtevant, J. M. *Proc. Natl. Acad. Sci. U.S.A.* **1976**, *73*, 3862.
- (7) Tristram-Nagle, S.; Nagle, J. F. *Chem. Phys. Lipids* **2004**, *127*, 3.
- (8) Nagle, J. F.; Wilkinson, D. A. *Biophys. J.* **1978**, *23*, 159.
- (9) Dietrich, C.; Bagatolli, L. A.; Volovyk, Z. N.; Thompson, N. L.; Levi, M.; Jacobson, K.; Gratton, E. *Biophys. J.* **2001**, *80*, 1417.
- (10) Szekely, P.; Dvir, T.; Asor, R.; Resh, R.; Steiner, A.; Szekely, O.; Ginsburg, A.; Mosenkis, J.; Guralnick, V.; Dan, Y.; Wolf, T.; Tamburu, C.; Raviv, U. *J. Phys. Chem. B* **2011**, *115*, 14501.
- (11) Kucerka, N.; Liu, Y. F.; Chu, N. J.; Petrache, H. I.; Tristram-Nagle, S. T.; Nagle, J. F. *Biophys. J.* **2005**, *88*, 2626.
- (12) Szekely, O.; Steiner, A.; Szekely, P.; Amit, E.; Asor, R.; Tamburu, C.; Raviv, U. *Langmuir* **2011**, *27*, 7419.
- (13) Szekely, O.; Schilt, Y.; Steiner, A.; Raviv, U. *Langmuir* **2011**, *27*, 14767.
- (14) Belitzky, A.; Melamed-Book, N.; Weiss, A.; Raviv, U. *Phys. Chem. Chem. Phys.* **2011**, *13*, 13809.
- (15) Flashner, E.; Raviv, U.; Friedler, A. *Biochem. Biophys. Res. Commun.* **2011**, *407*, 13.
- (16) Kraft, M. L.; Weber, P. K.; Longo, M. L.; Hutcheon, I. D.; Boxer, S. G. *Science* **2006**, *313*, 1948.
- (17) Cohen, J. A.; Podgornik, R.; Hansen, P. L.; Parsegian, V. A. *J. Phys. Chem. B* **2009**, *113*, 3709.
- (18) Szekely, P.; Ginsburg, A.; Ben-Nun, T.; Raviv, U. *Langmuir* **2010**, *26*, 13110.
- (19) Ben-Nun, T.; Ginsburg, A.; Szekely, P.; Raviv, U. *J. Appl. Crystallogr.* **2010**, *43*, 1522.
- (20) Nadler, M.; Steiner, A.; Dvir, T.; Szekely, O.; Szekely, P.; Ginsburg, A.; Asor, R.; Resh, R.; Tamburu, C.; Peres, M.; Raviv, U. *Soft Matter* **2011**, *7*, 1512.
- (21) Steiner, A.; Szekely, P.; Szekely, O.; Dvir, T.; Asor, R.; Yuval-Naeh, N.; Keren, N.; Kesselman, E.; Danino, D.; Resh, R.; Ginsburg, A.; Guralnik, V.; Feldblum, E.; Tamburu, C.; Peres, M.; Raviv, U. *Langmuir* **2012**, *28*, 2604.
- (22) Leneveu, D. M.; Rand, R. P.; Parsegian, V. A. *Nature* **1976**, *259*, 601.
- (23) Gordeliy, V. I.; Cherezov, V.; Teixeira, J. *Phys. Rev. E* **2005**, *72*.
- (24) Parsegian, V. A. *Van Der Waals Forces: A Handbook for Biologists, Chemists, Engineers and Physicists*; Cambridge University Press: New York, 2006.
- (25) Roux, D.; Safinya, C. R. *J. Phys.* **1988**, *49*, 307.
- (26) Szleifer, I.; Kramer, D.; Benshaul, A.; Gelbart, W. M.; Safran, S. A. *J. Chem. Phys.* **1990**, *92*, 6800.
- (27) Kucerka, N.; Nieh, M. P.; Katsaras, J. *Biochim. Biophys. Acta—Biomembr.* **2011**, *1808*, 2761.
- (28) Pan, J.; Tristram-Nagle, S.; Kucerka, N.; Nagle, J. F. *Biophys. J.* **2008**, *94*, 117.
- (29) Deme, B.; Dubois, M.; Gulik-Krzywicki, T.; Zemb, T. *Langmuir* **2002**, *18*, 997.
- (30) Chen, F. Y.; Hung, W. C.; Huang, H. W. *Phys. Rev. Lett.* **1997**, *79*, 4026.
- (31) Nagle, J. F.; Tristram-Nagle, S. *Biochim. Biophys. Acta—Rev. Biomembr.* **2000**, *1469*, 159.
- (32) Gordeliy, V. I.; Cherezov, V. G.; Teixeira, J. *J. Mol. Struct.* **1996**, *383*, 117.
- (33) Petrache, H. I.; Dodd, S. W.; Brown, M. F. *Biophys. J.* **2000**, *79*, 3172.
- (34) Nagle, J. F.; Petrache, H. I.; Gouliaev, N.; Tristram-Nagle, S.; Liu, Y. F.; Suter, R. M.; Gawrisch, K. *Phys. Rev. E* **1998**, *58*, 7769.
- (35) Mason, P. C.; Gaulin, B. D.; Epan, R. M.; Katsaras, J. *Phys. Rev. E* **2000**, *61*, 5634.
- (36) Chu, N.; Kucerka, N.; Liu, Y. F.; Tristram-Nagle, S.; Nagle, J. F. *Phys. Rev. E* **2005**, *71*, 041904.